Supporting Information for "North Atlantic cooling is slowing down mass loss of Icelandic glaciers"

Brice Noël[1], Guðfinna Aðalgeirsdóttir[2], Finnur Pálsson[2], Bert Wouters[1,3],

Stef Lhermitte[3], Jan M. Haacker[3], and Michiel R. van den Broeke[1]

[1]Institute for Marine and Atmospheric research Utrecht, Utrecht University, Utrecht, Netherlands.

[2]Institute of Earth Sciences, University of Iceland, Reykjavìk, Iceland.

[3]Department of Geoscience & Remote Sensing, Delft University of Technology, Delft, Netherlands.

Contents of this file

Introduction

1. Figure S1 shows Iceland surface elevation and bare ice albedo.

2. Figure S2 evaluates downscaled surface mass balance of Icelandic glaciers using in situ and remote sensing measurements. Near-surface temperature above Icelandic glaciers is also evaluated.

Corresponding author: B. Noël, Institute for Marine and Atmospheric research Utrecht, Utrecht University, Princetonplein 5, 3584 CC, Utrecht, Netherlands. (b.p.y.noel@uu.nl)

3. Figure S3 shows the spatial correlation between sea surface temperature and 2 m air temperature above Icelandic glaciers.

4. Figure S4 shows the spatial correlation between sea surface temperature and runoff from Icelandic glaciers.

5. Figure S5 shows the interaction between the regional cooling in the North Atlantic Ocean and the large-scale background warming.

6. Table S1 compares downscaled Icelandic glacier mass balance from this study with recent published estimates.

7. Table S2 lists the current and projected surface mass balance components of Icelandic glaciers throughout the 21st century.

References

Aðalgeirsdóttir, G., Pálsson, F., Thorsteinsson, T., Magnússon, E., Belart, J. M. C., Jóhannesson, T., ... Björnsson, H. (2020). Glacier changes in Iceland from 1890 to 2019. *Frontiers in Earth Science*, *8*(523646), 1 - 15. doi: 10.3389/feart.2020.523646

Björnsson, H., Pálsson, F., Gudmundsson, S., Magnússon, E., Aðalgeirsdóttir, G., Jóhannesson, T., ... Thorsteinsson, T. (2013). Contribution of Icelandic ice caps to sea level rise: Trends and variability since the Little Ice Age. *Geophysical Research Letters*, *40*(8), 1546 - 1550. doi: 10.1002/grl.50278

Box, J. E., Colgan, W. T., Wouters, B., Burgess, D. O., O'Neel, S., Thomson, L. I., & Mernild, S. H. (2018). Global sea-level contribution from Arctic land ice: 1971–2017. *Environmental Research Letters*, *13*(12), 125012. doi: 10.1088/1748-9326/aaf2ed

Ciraci, E., Velicogna, I., & Swenson, S. (2020). Continuity of the Mass Loss of the

World's Glaciers and IceCaps From the GRACE and GRACE Follow-On Missions. *Geophysical Research Letters*, *47*(9), e2019GL086926. doi: 10.1029/2019GL086926

Dee, D. P., Uppala, S. M., Simmons, A. J., Berrisford, P., Poli, P., Kobayashi, S., ... Vitart, F. (2011). The ERA-Interim reanalysis: configuration and performance of the data assimilation system. *Quarterly Journal of the Royal Meteorological Society*, *137*, 553 - 597. doi: 10.1002/qj.828

Foresta, L., Gourmelen, N., Pálsson, F., Nienow, P., Björnsson, H., & Shepherd, A. (2016). Surface elevation change and mass balance of Icelandic ice caps derived from swath mode CryoSat-2 altimetry. *Geophysical Research Letters*, *43*(23), 12,138 - 12,145. doi: 10.1002/2016GL071485

Gardner, A. S., Moholdt, G., Cogley, J. G., Wouters, B., Arendt, A. A., Wahr, J., ... Paul, F. (2013). A reconciled estimate of glacier contributions to sea level rise: 2003 to 2009. *Science*, *340*(6134), 852 - 857. doi: 10.1126/science.1234532

Hersbach, H., Bell, B., Berrisford, P., Hirahara, S., Horànyi, A., Munoz-Sabater, J., ... Thépaut, J. (2020). The ERA5 global reanalysis. *Quarterly Journal of the Royal Meteorological Society*, *146*(730), 1999 - 2049. doi: 10.1002/qj.3803

Hock, R., Rasul, G., Adler, C., Cáceres, B., Gruber, S., Hirabayashi, Y., ... Steltzer, H. (2019). *High mountain areas. in: Ipcc special report on the ocean and cryosphere in a changing climate.* IPCC SROCC.

Jacob, T., Wahr, J., Pfeffer, W. T., & Swenson, S. (2012). Recent contributions of glaciers and ice caps to sea level rise. *Nature*, *514*(482), 514 - 518. doi: 10.1038/nature10847

Jóhannesson, T., Pálmason, B., Hjartarson, A., Jarosch, A. H., Magnússon, E., Belart,

J. M. C., & Gudmundsson, M. T. (2020). Non-surface mass balance of glaciers in Iceland. *Journal of Glaciology*, *66*(258), 685 -697. doi: 10.1017/jog.2020.37

Nilsson, J., Sørensen, L. S., Barletta, V. R., & Forsberg, R. (2015). Mass changes in Arctic ice caps and glaciers: implications of regionalizing elevation changes. *The Cryosphere*, *9*(1), 139 - 150. doi: 10.5194/tc-9-139-2015

Porter, C., Morin, P., Howat, I., Noh, M.-J., Bates, B., Peterman, K., ... Bojesen, M. (2018). *ArcticDEM.* Harvard Dataverse. Retrieved from {https://doi.org/10.7910/DVN/OHHUKH} doi: 10.7910/DVN/OHHUKH

RGI Consortium. (2017). *Randolph Glacier Inventory–A Dataset of Global Glacier Outlines: Version 6.0: Technical Report.* Global Land Ice Measurements from Space. Retrieved from {https://doi.org/10.7265/N5-RGI-60} doi: 10.7265/N5-RGI-60

Schrama, E., Wouters, B., & Rietbroek, R. (2014). A mascon approach to assess ice sheet and glacier mass balances and their uncertainties from GRACE data. *Journal of Geophysical Research*, *119*(7), 6048 - 6066. doi: 10.1002/2013JB010923

Siemes, C., Ditmar, P., Riva, R. E. M., Slobbe, D. C., Liu, X. L., & Farahani, H. H. (2013). Estimation of mass change trends in the Earth's system on the basis of GRACE satellite data, with application to Greenland. *Journal of Geodesy*, *87*, 69 - 87. doi: 10.1007/s00190-012-0580-5

Sørensen, L. S., Jarosch, A. H., Aðalgeirsdóttir, G., Barletta, V. R., Forsberg, R., Pálsson, F., ... Jóhannesson, T. (2017). The effect of signal leakage and glacial isostatic rebound on GRACE-derived ice mass changes in Iceland. *209*, *1*, 226 - 233. doi: 10.1093/gji/ggx008

Uppala, S. M., Kållberg, P. W., Simmons, A. J., Andrae, U., Bechtold, V. D. C., Fiorino, M., … Woollen, J. (2005). The ERA-40 re-analysis. *Quarterly Journal of the Royal Meteorological Society*, *131*, 2961 - 3012.

Von Hippel, M., & Harig, C. (2019). Long-Term and Inter-annual Mass Changes in the Iceland Ice Cap Determined From GRACE Gravity Using Slepian Functions. *Frontiers in Earth Science*, *7*(171), 1 - 10. doi: 10.3389/feart.2019.00171

Wouters, B., Chambers, D., & Schrama, E. J. O. (2008). GRACE observes small-scale mass loss in Greenland. *Geophysical Research Letters*, *35*(20), L20501. doi: 10.1029/2008GL034816

Wouters, B., Gardner, A., & Moholdt, G. (2019). Global Glacier Mass Loss During the GRACE Satellite Mission (2002-2016). *Frontiers in Earth Sicence*, *7*(96), 11 p. doi: 10.3389/feart.2019.00096

Zemp, M., Huss, M., Thibert, E., Eckert, N., McNabb, R., Huber, J., … Cogley, J. G. (2019). Global glacier mass changes and their contributions to sea-level rise from 1961 to 2016. *Nature*, *568*, 382 - 386. doi: 10.1038/s41586-019-1071-0

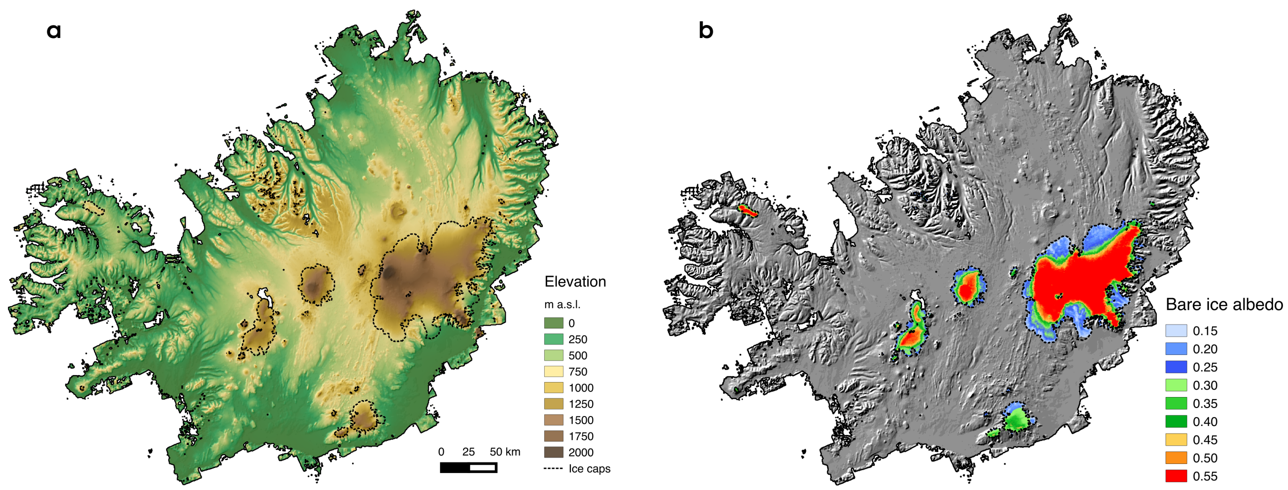

Figure S1. **a** Surface elevation derived from the ArcticDEM at 100 m horizontal resolution re-sampled to a 500 m grid (Porter et al., 2018). **b** Bare ice albedo derived from MODIS imagery at 500 m resolution and averaged for the period 2000-2019. Dashed line outlines the ice mask of Iceland derived from the Randolph Glacier Inventory version 6 (RGI Consortium, 2017).

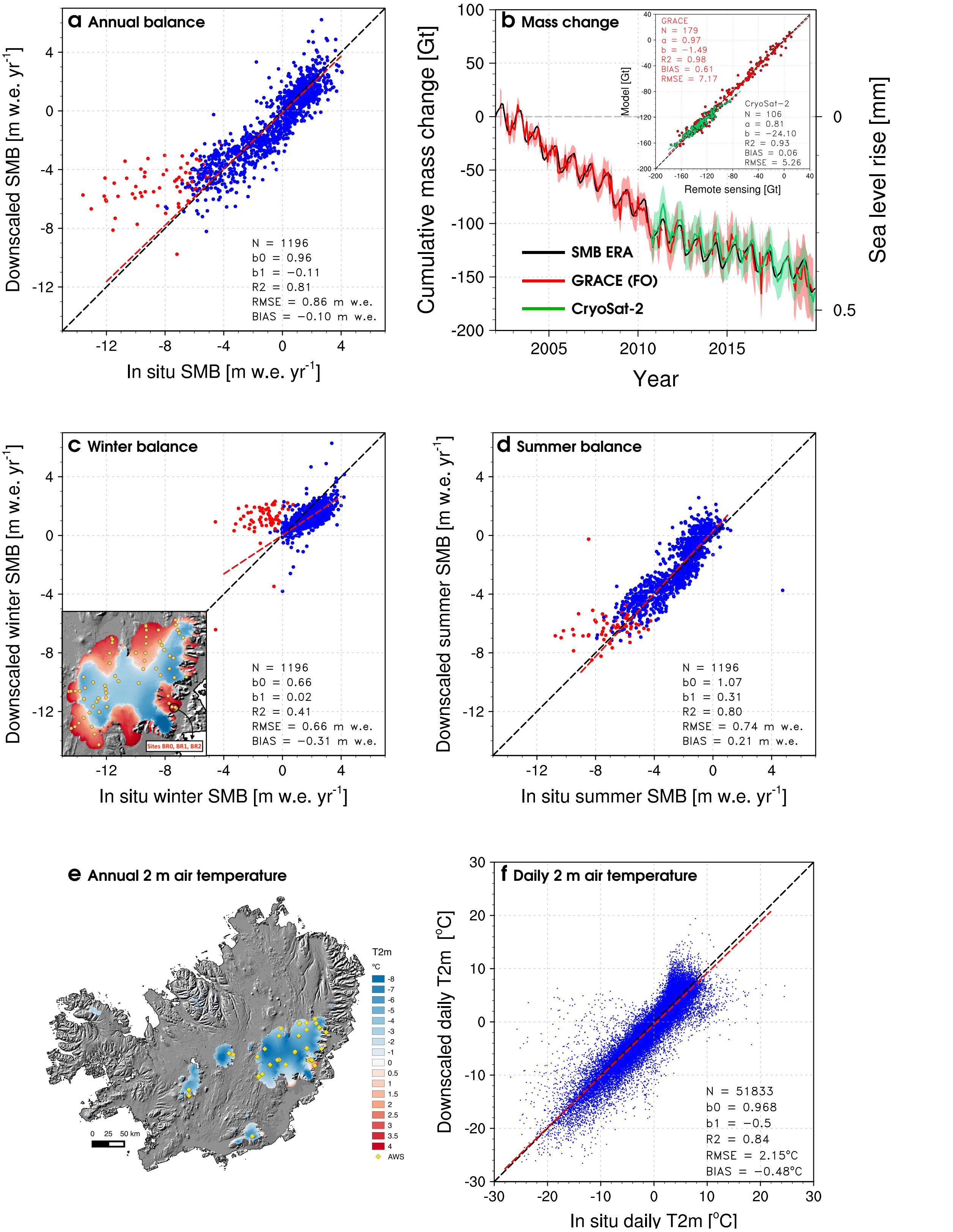
a Annual balance
N = 1196
b0 = 0.96
b1 = −0.11
R2 = 0.81
RMSE = 0.86 m w.e.
BIAS = −0.10 m w.e.
Downscaled SMB [m w.e. yr-1]
In situ SMB [m w.e. yr-1]
b Mass change
GRACE
N = 179
a = 0.97
b = −1.49
R2 = 0.98
BIAS = 0.61
RMSE = 7.17
CryoSat−2
N = 106
a = 0.81
b = −24.10
R2 = 0.93
BIAS = 0.06
RMSE = 5.26
Model [Gt]
Remote sensing [Gt]
SMB ERA
GRACE (FO)
CryoSat-2
Cumulative mass change [Gt]
Sea level rise [mm]
Year
c Winter balance
N = 1196
b0 = 0.66
b1 = 0.02
R2 = 0.41
RMSE = 0.66 m w.e.
BIAS = −0.31 m w.e.
Sites BR0, BR1, BR2
Downscaled winter SMB [m w.e. yr-1]
In situ winter SMB [m w.e. yr-1]
d Summer balance
N = 1196
b0 = 1.07
b1 = 0.31
R2 = 0.80
RMSE = 0.74 m w.e.
BIAS = 0.21 m w.e.
Downscaled summer SMB [m w.e. yr-1]
In situ summer SMB [m w.e. yr-1]
e Annual 2 m air temperature
T2m
°C
AWS
0 25 50 km
f Daily 2 m air temperature
N = 51833
b0 = 0.968
b1 = −0.5
R2 = 0.84
RMSE = 2.15°C
BIAS = −0.48°C
Downscaled daily T2m [°C]
In situ daily T2m [°C]

Figure S2. **a** Comparison between modelled and observed annual SMB collected at ∼65 stakes across Vatnajökull ice cap (yellow dots in Fig. S2c). The red dashed line represents the regression excluding three sites in southeast Vatnajökull, namely BR0-BR1-BR2 (red dots), outlined on the inset map of Fig. S2c. **b** Time series of monthly cumulative SMB overlapping the satellite period (2002-2019) and including records from GRACE (2002-2016), GRACE-FO (2018-2019) and CryoSat-2 (2011-2019). The inset shows the correlation between modelled mass change from RACMO2.3-ERA at 500 m resolution and GRACE (red dots) and CryoSat-2 (green dots). **c** and **d** same as **a** but for the winter (September-May) and summer (May-September) balance respectively. Statistics including the number of observations (N), slope (b0) and intercept (b1) of the regression line, coefficient of determination (R^2), RMSE and mean bias between model and observations are also listed. In **a**, **c** and **d**, statistics exclude the three sites defined above. For a meaningful comparison with stakes that do not measure internal accumulation in firn, we subtract modelled refreezing to the downscaled SMB in the accumulation zone (**a**, **c** and **d**). Note that modelled cumulative mass change in **b** does not consider non-surface mass balance processes such as basal melt and calving (Jóhannesson et al., 2020). **e** Modelled annual mean 2 m air temperature (T2m) above Icelandic glaciers (1958-2019). Yellow dots locate 27 automatic weather stations (AWS) installed on the four main ice caps in the summer of 1994-2019. **f** Comparison between daily modelled and measured T2m collected at 27 AWS (Fig. S2e) for the period 1994-2019. Relevant statistics including all measurements are also listed.

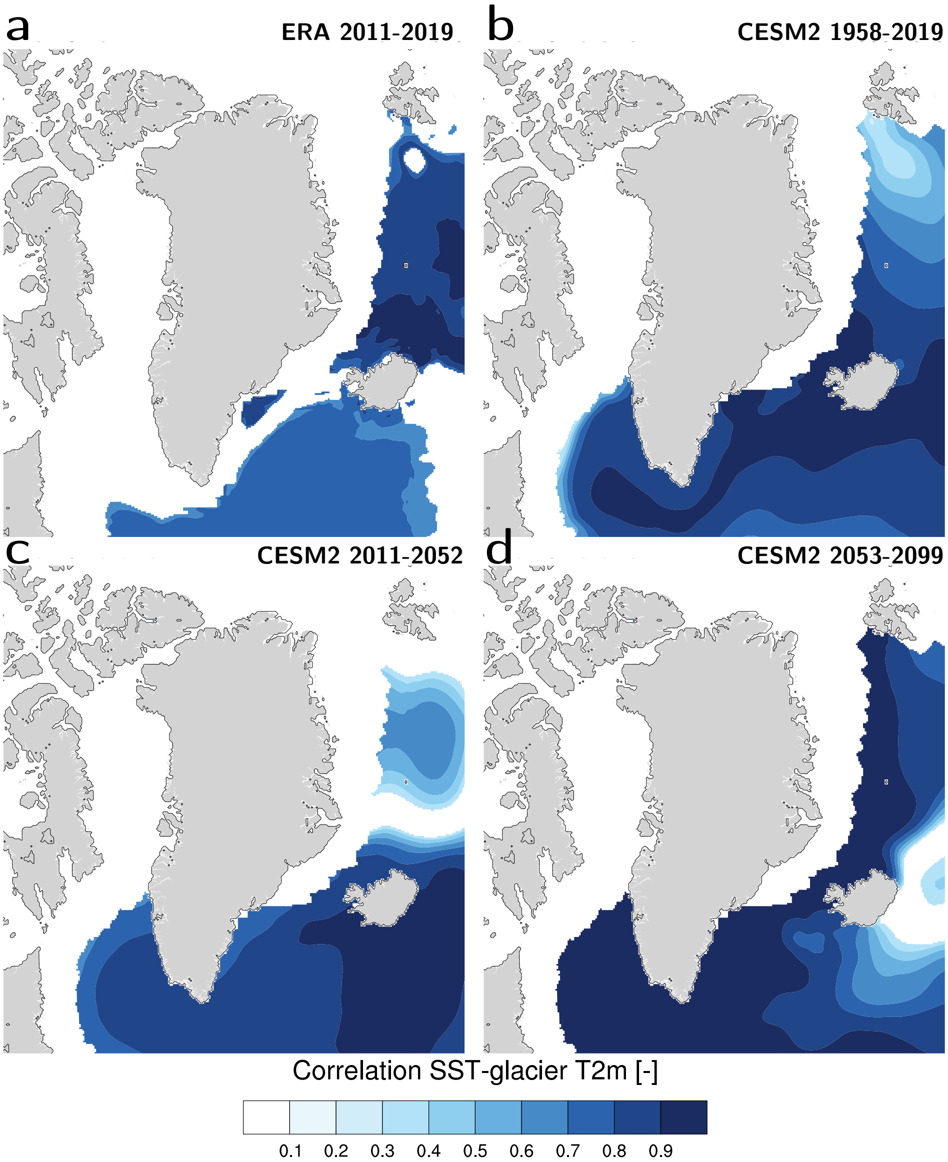

Figure S3. Spatial correlation between sea surface temperature (SST) in the North Atlantic Ocean and Iceland glacier 2 m air temperature (T2m) for **a** RACMO2.3-ERA in 2011-2019, and RACMO2.3-CESM2 for the periods **b** 1958-2019, **c** 2011-2052 and **d** 2053-2099. In **a** North Atlantic SST is derived from observational ERA reanalyses (Uppala et al., 2005; Dee et al., 2011; Hersbach et al., 2020). In **b-d** North Atlantic SST is derived from the earth system model CESM2. Only sea-ice free pixels were considered, as determined from ERA reanalyses. To highlight spatial patterns, the correlation maps are expressed as absolute values and only significant correlations are shown ($P < 0.05$).

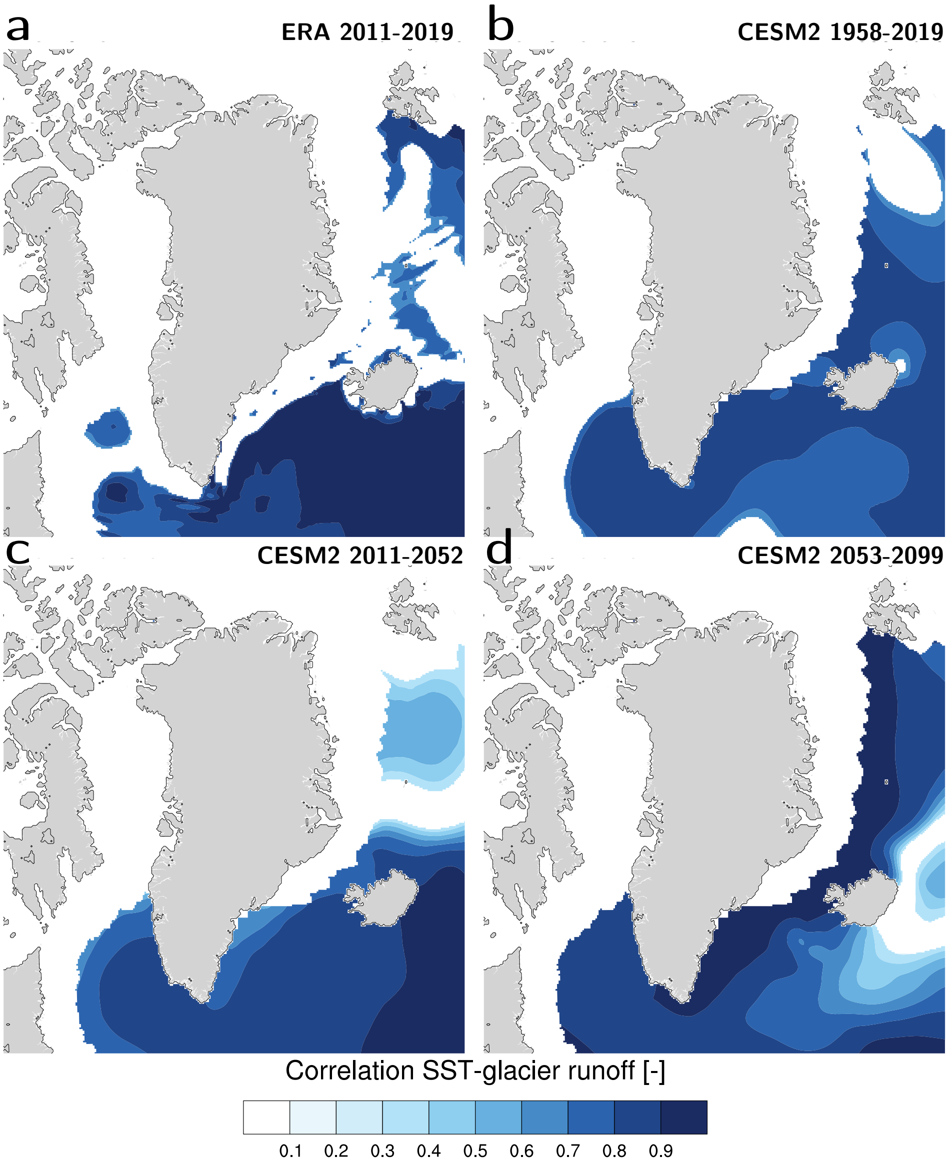

Figure S4. Spatial correlation between sea surface temperature (SST) in the North Atlantic Ocean and Iceland glacier-integrated runoff at 500 m resolution as modelled by **a** RACMO2.3-ERA in 2011-2019, and RACMO2.3-CESM2 for the periods **b** 1958-2019, **c** 2011-2052 and **d** 2053-2099. In **a** North Atlantic SST is derived from observational ERA reanalyses (Uppala et al., 2005; Dee et al., 2011; Hersbach et al., 2020). In **b-d** North Atlantic SST is derived from the earth system model CESM2. Only sea-ice free pixels were considered, as determined from ERA reanalyses. To highlight spatial patterns, the correlation maps are expressed as absolute values and only significant correlations are shown ($P < 0.05$).

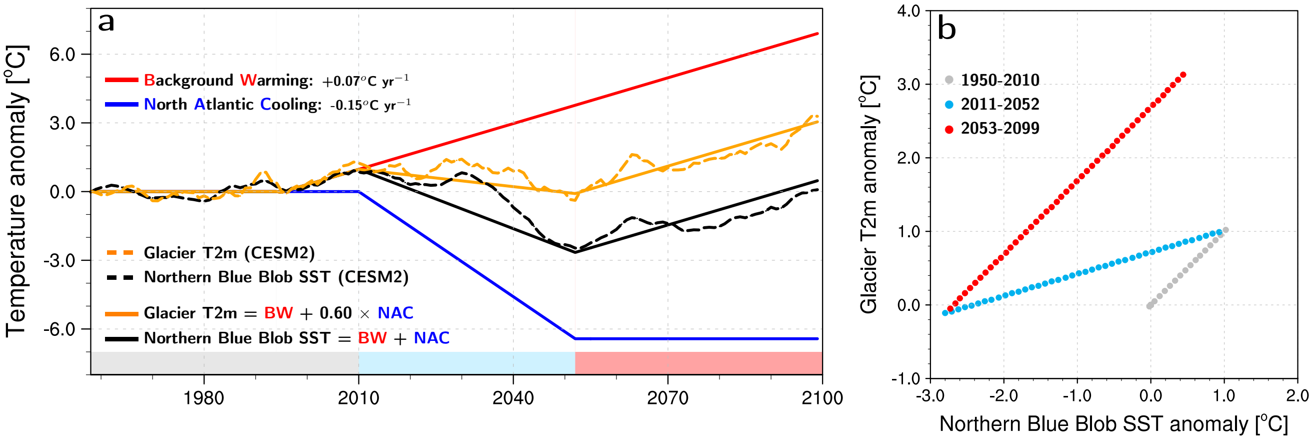

Figure S5. **a** Idealised decomposition of the projected anomalies in Northern Blue Blob (NBB) sea surface temperature (SST; dashed black line) and glacier 2 m air temperature (T2m; dashed orange line) into two opposite temperature signals: a large-scale Background Warming (BW; red line) and regional North Atlantic Cooling (NAC; blue line). BW is estimated as a linear regression of the glacier T2m warming in the period 1995-2010 (+0.07 ^{o}C yr^{-1}). NAC is estimated as the strongest cooling trend observed in the NBB in the period 2011-2019 (-0.15 ^{o}C yr^{-1} in Fig. 3a). Idealised NBB SST (solid black line) is reproduced by summing the BW and NAC signals. Assuming that the advection of air masses from the NBB to Iceland dissipates 40% of the initial signal, glacier T2m is reproduced by summing the full atmospheric BW and the remaining 60% NAC signal. This explains the asymmetrical cooling that is stronger in the NBB (black lines) than for glacier T2m (orange lines). **b** Correlation between idealised NBB SST (solid black line in **a**) and glacier T2m (solid orange line in **a**). The asymmetrical cooling between NBB SST and glacier T2m leads to an asymmetrical correlation (z-shaped) similar to Fig. 2c. Coloured dots represent the three key mass balance stages: 1958-2010 (grey), 2011-2052 (cyan) and 2053-2099 (red).

Table S1. Comparison between mass balance (SMB) from the current study and independent in situ and remotely sensed mass change estimates. Note that the modelled mass balance does not consider non-surface mass balance processes such as basal melt and calving (Jóhannesson et al., 2020).

References	Method	Period	Units	Estimate	This study
Wouters et al. (2008)	Satellite gravimetry	2003-2008	Gt yr^{-1}	-8.9 ± 3.0	-10.5 ± 2.5
Siemes et al. (2013)	Satellite gravimetry	2003-2008	Gt yr^{-1}	-17.0 ± 9.0	-10.5 ± 2.5
Gardner et al. (2013)	Satellite gravimetry	2003-2009	Gt yr^{-1}	-10.0 ± 2.0	-11.2 ± 2.5
Jacob et al. (2012)	Satellite gravimetry	2003-2010	Gt yr^{-1}	-11.0 ± 2.0	-12.8 ± 2.5
Sørensen et al. (2017)	Satellite gravimetry	2003-2010	Gt yr^{-1}	-11.4 ± 2.2	-12.8 ± 2.5
Schrama et al. (2014)	Satellite gravimetry	2003-2013	Gt yr^{-1}	-8.6 ± 0.6	-11.1 ± 2.5
Box et al. (2018)	Satellite gravimetry	2003-2015	Gt yr^{-1}	-11.0 ± 5.0	-9.2 ± 2.5
Wouters et al. (2019)	Satellite gravimetry	2003-2016	Gt yr^{-1}	-10.0 ± 2.0	-9.3 ± 2.5
Von Hippel and Harig (2019)	Satellite gravimetry	2003-2016	Gt yr^{-1}	-9.3 ± 1.0	-9.3 ± 2.5
Ciraci et al. (2020)	Satellite gravimetry	2003-2019	Gt yr^{-1}	-15.9 ± 4.0	-8.8 ± 2.5
Nilsson et al. (2015)	Satellite altimetry	2003-2009	Gt yr^{-1}	-9.8 ± 2.8	-11.2 ± 2.5
Foresta et al. (2016)	Satellite altimetry	2010-2015	Gt yr^{-1}	-5.8 ± 0.7	-6.8 ± 2.5
Aðalgeirsdóttir et al. (2020)	Mixed methods	1980-1994	Gt yr^{-1}	1.5 ± 1.0	-2.6 ± 2.5
Aðalgeirsdóttir et al. (2020)	Mixed methods	1994-2010	Gt yr^{-1}	-11.6 ± 0.8	-10.2 ± 2.5
Aðalgeirsdóttir et al. (2020)	Mixed methods	1994-2019	Gt yr^{-1}	-9.6 ± 0.8	-8.5 ± 2.5
Aðalgeirsdóttir et al. (2020)	Mixed methods	1970-2019	Gt yr^{-1}	-4.3 ± 1.0	-4.9 ± 2.5
Aðalgeirsdóttir et al. (2020)	Mixed methods	1992-2019	Gt yr^{-1}	-8.3 ± 0.8	-7.7 ± 2.5
Aðalgeirsdóttir et al. (2020)	Mixed methods	2005-2019	Gt yr^{-1}	-7.6 ± 0.8	-8.3 ± 2.5
Björnsson et al. (2013)	Mixed methods	1995-2010	Gt yr^{-1}	-9.5 ± 1.5	-10.7 ± 2.5
Björnsson et al. (2013)	Mixed methods	2003-2010	Gt yr^{-1}	-11.0 ± 2.0	-12.8 ± 2.5
Zemp et al. (2019)	Mixed methods	2006-2016	Gt yr^{-1}	-5.0 ± 4.0	-8.5 ± 2.5
Hock et al. (2019)	Mixed methods	2006-2016	Gt yr^{-1}	-7.0 ± 3.0	-6.8 ± 2.5

Table S2. This table lists the surface mass balance (SMB) and components (top) from the RACMO2.3-ERA simulation averaged for the periods 1958-1994, 1995-2010 and 2011-2019; (bottom) from RACMO2.3-CESM2 under a SSP5-8.5 warming scenario averaged for the periods 1958-2010, 2011-2052 and 2053-2099.

ERA	Units	SMB	Snowfall	Rainfall	Runoff	Melt	Refreezing
1958-1994	Gt yr^{-1}	-1.2 $\pm$ 2.5	22.4	6.0	29.8	35.7	11.9
1995-2010	Gt yr^{-1}	-10.7 $\pm$ 2.5	20.4	7.0	38.4	43.5	12.1
2011-2019	Gt yr^{-1}	-5.3 $\pm$ 2.5	22.4	7.0	35.1	38.6	10.5
SSP5-8.5	Units	SMB	Snowfall	Rainfall	Runoff	Melt	Refreezing
1958-2010	Gt yr^{-1}	-4.0 $\pm$ 2.5	21.8	6.3	32.4	38.1	12.0
2011-2052	Gt yr^{-1}	-4.8 $\pm$ 2.5	22.3	8.7	36.4	37.8	10.1
2053-2099	Gt yr^{-1}	-13.9 $\pm$ 2.5	19.0	8.4	42.2	42.1	8.3